

## DYNAMIC AMPLIFICATIONS OF TORSIONALLY UNBALANCED BASE-ISOLATED STRUCTURES

A. Tena-Colunga<sup>1</sup> and J.L. Escamilla-Cruz<sup>2</sup>

<sup>1</sup> Professor, Departamento de Materiales, Universidad Autónoma Metropolitana, Mexico City, Mexico

<sup>2</sup> Structural Engineer, CH2MHill, Mexico City, Mexico

Email: atc@correo.azc.uam.mx, josescamc75@hotmail.com

### ABSTRACT

The torsional response of base-isolated structures with bilinear hysteretic behavior when eccentricities are set in the superstructure is presented. Nonlinear dynamic analyses were used to study peak responses for different ratios of the static eccentricities ( $e_s$ ) between the centers of mass and the centers of rigidity of the superstructure, due to asymmetries in the stiffnesses of the structural elements. Among other relevant issues, it was found that torsional amplifications due to an asymmetric distribution of the masses in the superstructure are higher than those due to asymmetries in the stiffnesses of the structural elements for all the  $T_1/T_b$  ratios considered in the effective base-isolated period range under consideration.

**KEYWORDS:** torsional response, seismic isolation, base-isolated structures, elastomeric bearings, displacement ductility demands, static eccentricities

### 1. INTRODUCTION

It is well known that torsion adversely affects the response of conventional structures, as well as base isolated structures. Therefore, for design purposes, it would be desirable to restrict in building codes the use of static or simplified dynamic methods of analysis and design for base-isolated structures susceptible of torsional responses based upon simple parameters that most structural engineers can easily assess, recognizing this condition of structural irregularity.

Because 42% percent of the collapses that occurred in Mexico City during the 1985 earthquake were related to torsional response of asymmetric buildings, Mexico's Federal District Code introduced this design philosophy for conventional structures since 1987, and other Mexican model codes such as the Manual of Civil Structures share this philosophy since 1993. According to RCDF-2004, buildings where torsional plan eccentricities ( $e_s$ ) computed for any story from static seismic analysis exceed 10 percent of the plan dimension in the given direction of analysis must be considered and designed as irregular structures and, if  $e_s$  is 20 percent or higher, they must be designed as strongly irregular structures. However, other state-of-the-art seismic codes worldwide do not restrict the use of static and simplified dynamic methods of analysis for structures susceptible of torsional responses, particularly their guidelines for base-isolated structures.

During the development of guidelines for the seismic design of base isolated structures for Mexico (i.e., Tena-Colunga 2005) it was considered to be very important that they were compatible with the general design philosophy of the seismic codes of Mexico. Therefore, defining specific target values for static eccentricities for the superstructure ( $e_s$ ) and for the isolation system ( $e_b$ ) was crucial. These target values would allow to determine when expected design displacements for the isolation system associated with the guidelines are not well covered as compared to rigorous nonlinear dynamic analyses. These target values are needed to restrict the use of static or simplified dynamic methods of analysis and design.

Comprehensive parametric studies were started covering the period range  $1.5s \leq T_1 \leq 3s$ , as they were of utmost importance for the seismic design of base-isolated structures from a code development viewpoint. Previous studies conducted by the first author covered them when eccentricities were set in the superstructure (mass

eccentricity, Tena-Colunga and Gómez-Soberón 2002) and in the isolation system (Tena-Colunga and Zambrana-Rojas 2006).

Despite the fact that the described research was extensive, additional parametric studies were needed to evaluate the impact of other two important parameters. First, it was necessary to assess the impact in torsional amplifications of the  $T_I/T_s$  ratio, a recognized important parameter for the design of base-isolated structures. For example, it is recommended in the New Zealand practice that the effective period of the isolated structure at the design displacement,  $T_I$ , should be greater than two times the elastic, fixed-base period of the structure above the isolation system,  $T_s$ , this is,  $T_I/T_s \geq 2$ , whereas in U.S. guidelines such as UBC-97, IBC-06 and ASCE 7-05 it is required that  $T_I/T_s \geq 3$  in order to use the static method for seismic analysis. Second, it was important to assess for the period range of interest and different  $T_I/T_s$  ratios the relative differences in the torsional amplifications when asymmetries in the superstructure are due to: (a) mass eccentricities or, b) stiffness eccentricities.

Therefore, a comprehensive study (Escamilla-Cruz 2005) was started to discern how the parameters described above impact specific helpful design parameters for isolators, such as: (1) displacement ductility demands, (2) peak displacements, (3) amplification factors due to bidirectional seismic input (with respect to unidirectional input) and, (4) amplification factors because of bidirectional eccentricity (with respect to unidirectional eccentricity). For space constraints, this paper only summarizes the following results which are important from a code development perspective: (a) amplifications of asymmetric systems with respect to counterpart symmetric systems of reference and, (b) relative amplifications of asymmetric systems with mass eccentricities with respect to asymmetric systems with stiffness eccentricities.

## 2. STRUCTURAL MODELS CONSIDERED

In order to assess the impact of different  $T_I/T_s$  ratios in the torsional amplifications for isolators, four different three-story building models (Figs. 1 and 2) were designed as benchmark symmetric models to obtained fundamental fixed-base periods  $T_s = 0.187s, 0.5s, 0.75s$  and  $1.2s$ . All benchmark buildings: a) are regular in elevation and symmetric with respect to two main orthogonal axes and, b) have four frames in each direction with a typical bay width of 7m and a story height of 3m. Typical RC columns are of square cross section and typical RC beams are rectangular, where  $f'_c = 250 \text{ kg/cm}^2$ . Buildings are supported by 16 elastomeric bearings, one below a rigid slab along each column line (Figs. 1 and 2). Braces of A-36 steel are located as shown in Figs. 1 and 2 and are of square box section.

Typical sections of these benchmark models are shown in Table 1. As it can be deduced from Table 1, target fixed-base periods  $T_s$  were obtained by modifying the  $E_c I$  stiffness of RC beams and columns, as well the cross section of the steel bracing. It is worth noting that the values identified for Young Moduli  $E_c$  in Table 1 are consistent with those proposed by the concrete norms of Mexico's Federal District Code from 1976 to 2004.

Table 1. General dimensions and properties for the structures above the isolation system						
Model	$T_s$ (s)	$\Omega_{\theta s}$	Reinforced Concrete Elements			Steel Elements
			Columns (cm)	Beams (cm)	$E_c$ (kg/cm <sup>2</sup> )	Braces (cm)
SBA1M	0.187	1.2	65x65	35x75	$14,000\sqrt{f'_c}$	25x25x0.8
SBA2M	0.5	0.8	55x55	35x60	$10,000\sqrt{f'_c}$	15x15x0.68
SBA3M	0.75	0.8	46x46	25x53	$8,000\sqrt{f'_c}$	15x15x0.65
SBA4M	1.2	0.8	36x36	20x42	$8,000\sqrt{f'_c}$	15x15x0.52

In order to assess the torsional to lateral frequency ratio ( $\Omega_{\theta s}$ ) for the superstructure, the spatial position of the bracing was varied, as it can be observed in plan by comparing Figures 1 and 2. A torsionally stiff structure is

obtained when braces are placed in the perimeter (Fig. 1,  $\Omega_{0s}=1.2$ ) whereas a torsionally flexible structure is obtained when braces are placed in the central zone (Fig. 2,  $\Omega_{0s}=0.8$ ).

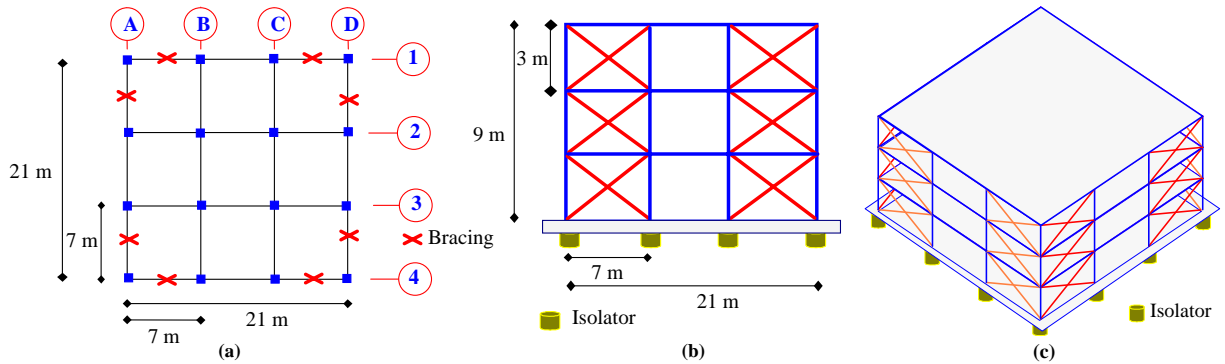


Figure 1. Benchmark models SBA1 and SBA1M, (a) Plan, (b) Elevation and, (c) 3D Layout.

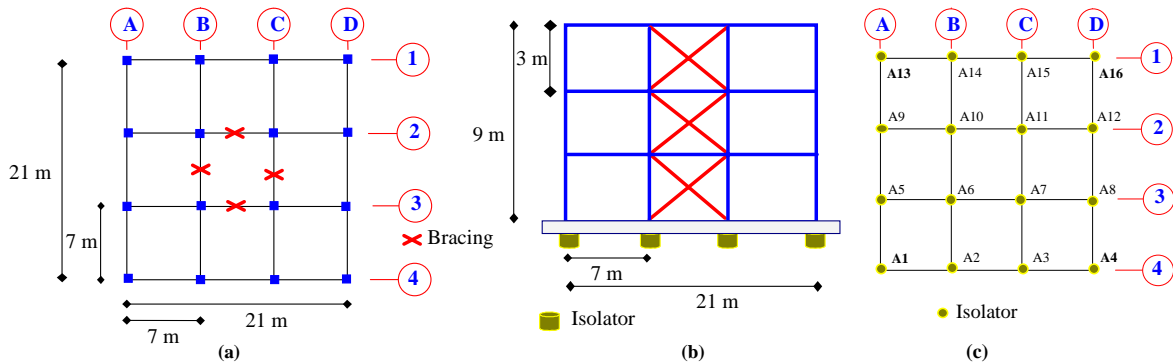


Figure 2. Benchmark models SBA2 SBA2M, SBA3, SBA3M, SBA4 and SBA4M, (a) Plan, (b) Elevation and, (c) Isolation system.

Because in this parametric study the smallest effective period for the base-isolated structure is  $T_I=1.5s$  and the maximum value is  $T_I=3s$ , this implies that the  $T_I/T_s$  ratios are within the following range: (a)  $8 < T_I/T_s \leq 16$  for  $T_s=0.187s$  ( $\Omega_{0s}=1.2$ ), (b)  $3 \leq T_I/T_s \leq 6$  for  $T_s=0.5s$  ( $\Omega_{0s}=0.8$ ), (c)  $2 \leq T_I/T_s \leq 4$  for  $T_s=0.75s$  ( $\Omega_{0s}=0.8$ ) and, (d)  $1.25 \leq T_I/T_s \leq 2.5$  for  $T_s=1.2s$  ( $\Omega_{0s}=0.8$ ).

The benchmark symmetric superstructure identified as SBA1M with  $T_s=0.187s$  and  $\Omega_{0s}=1.2$  is the structure that have been used in previous studies (Tena-Colunga and Gómez-Soberón 2002, Tena-Colunga and Zambrana-Rojas 2006). The benchmark symmetric superstructure identified as SBA2M with  $T_s=0.5s$  and  $\Omega_{0s}=0.8$  was designed to indirectly assess the requirement of U.S. codes where  $T_I/T_s \geq 3$  in order to use the static method for seismic analysis. The benchmark symmetric superstructure identified as SBA3M with  $T_s=0.75s$  and  $\Omega_{0s}=0.8$  was designed to indirectly assess the recommendation of the New Zealand practice where  $T_I/T_s \geq 2$  for base-isolated structures to prevent higher mode effects and dynamic amplifications due to the coupling of the base-isolated fundamental mode with the fundamental mode for the superstructure. Finally, the benchmark symmetric superstructure identified as SBA4M with  $T_s=1.2s$  and  $\Omega_{0s}=0.8$  was designed as a model with similar dynamic properties ( $T_s=1.2s$ ,  $\Omega_{0s}=0.8$  and  $T_I=2.12s$ ) to one previously studied by Nagarajaiah *et al.* (1993), where they obtained the highest torsional amplifications. It is worth noting that for the model used by Nagarajaiah *et al.* (1993)  $T_I/T_s = 2.12/1.2 = 1.77 < 2$ , below what is the minimum recommended by the New Zealand experience.

Static eccentricities in the superstructure ( $e_s$ ) of 5%, 10%, 15% and 20% the floor plan dimension ( $L=21m$ ) were selected, for both one direction and acting on a 45° angle, plus the completely symmetric case ( $e_s=0\%$ ), as

depicted in Figure 3 for the models with mass eccentricities and in Figure 4 for the models with stiffness eccentricities.

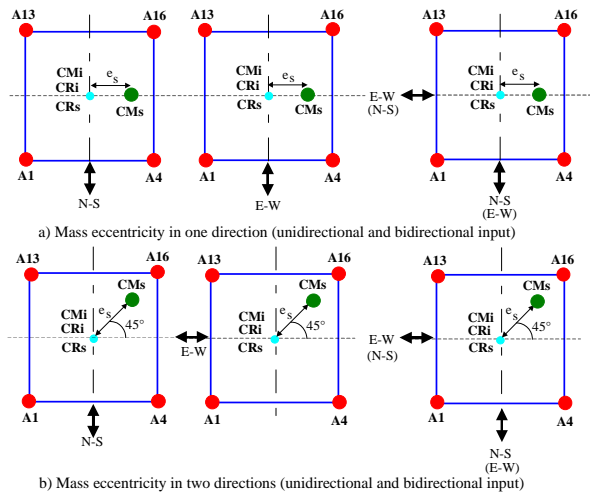


Figure 3. Definition of static eccentricities in the superstructure,  $e_s$ , due to mass eccentricities.

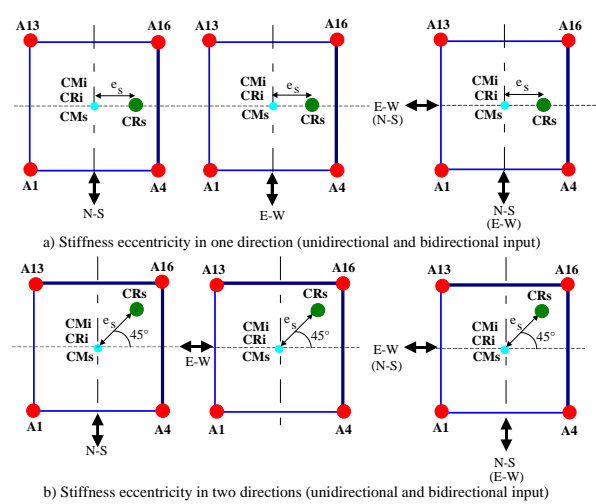


Figure 4. Definition of static eccentricities in the superstructure,  $e_s$ , due to stiffness eccentricities (stiffer perimeter frames are identified with a thick solid line).

Models where asymmetries in the superstructure are due to the change of the position of the centers of mass are identified as SBA1M, SBA2M, SBA3M and SBA4M. The static eccentricities  $e_s$  were obtained by shifting the centers of mass of the superstructure (CMs) from the center of stiffness of the superstructure (CRs), that are located in the geometric center of the plan, as depicted in Figure 3. For these models, the dynamic properties correspond to those reported in Table 1.

Models where asymmetries in the superstructure are due to changes in the lateral stiffness of the resisting braced frames are identified as SBA1, SBA2, SBA3 and SBA4. The static eccentricities  $e_s$  were obtained by shifting the centers of stiffness of the superstructure (CRs) from the centers of mass of the superstructure (CMs), that are located in the geometric center of the plan, as depicted in Figure 4. In order to shift the centers of stiffness of the superstructure (CRs), the stiffness properties of perimeter frames 1 and D (Figs. 1a and 2a) and those of the exterior braces of axis 2 and C (Fig. 2a) were modified until reaching the target  $e_s$  value using an iterative procedure based on the matricial method proposed by Damy which is described elsewhere (Tena-Colunga and Pérez-Osornio 2002). As a consequence,  $T_s$  and  $\Omega_{0s}$  ratios were slightly modified, as reported in detail in Escamilla-Cruz (2005). For example, for static eccentricities in two directions,  $T_s$  ranged from 0.182s for  $e_s=5\%$  to 0.177s for  $e_s=20\%$  for SBA1 models; 0.544s for  $e_s=5\%$  to 0.529s for  $e_s=20\%$  for SBA2 models, 0.827s for  $e_s=5\%$  to 0.802s for  $e_s=20\%$  for SBA3 models, and 1.327s for  $e_s=5\%$  to 1.29s for  $e_s=20\%$  for SBA4 models. For static eccentricities in one direction, variations were much smaller.

### 3. SELECTED ACCELERATION RECORDS

The same set of accelerograms used in previous studies, typical of strong subduction earthquakes recorded in firm soil sites or rock during the past two decades in the Mexican Pacific Coast were used in the present study. The two horizontal components of the following records were considered: (a) La Unión station (UNION), recorded during the September 19, 1985 Michoacán earthquake ( $M_s=8.1$ ), (b) San Marcos station (SMRZA), epicentral records for the April 25, 1989 earthquake ( $M_s=6.9$ ) and, (c) Termoeléctrica station (TMANZ), accelerograms with site effects recorded during the October 9, 1995 Manzanillo earthquake ( $M_w=8.0$ ). Some characteristics of the records are summarized in Table 2.

**Table 2. Some characteristics of the selected earthquake records**

STATION	Length of records (s)	E-W Record			N-S Record		
		$A_{max}$ (cm/s <sup>2</sup> )	$V_{max}$ (cm/s)	Strong motion Duration (s)	$A_{max}$ (cm/s <sup>2</sup> )	$V_{max}$ (cm/s)	Strong motion Duration (s)
UNION	62.3	127	12.6	26.4	174	21.0	24.2
SMRZ	30.4	148	16.7	6.47	165	17.7	5.03
TMANZ	154.6	387	30.7	38.8	381	28.9	45.6

#### 4. CHARACTERISTICS OF BILINEAR ISOLATORS

As in previous studies, bilinear isolators with a post to pre yielding stiffness of 10% ( $k_2/k_1=0.10$ ) were selected. The general mechanical properties for the isolators were defined following some available recommendations of the New Zealand practice and the 1997 Uniform Building Code now adapted in the proposed Mexican guidelines, as described in greater detail elsewhere (Tena-Colunga 2005).

#### 5. GENERALITIES OF PARAMETRIC STUDIES

As in previous studies, the effective period range  $1.5s \leq T_1 \leq 3s$  was selected to study the influence of static torsional eccentricities (mass-related or stiffness-related) on the dynamic response of base-isolated structures. Nonlinear dynamic responses of base-isolated models were computed in the selected effective period range with a period increment of 0.1 second, this is, there were 16 models in the period range  $1.5s \leq T_1 \leq 3s$ . A yield strength ratio  $V_y/W=0.05$  for the isolation system was considered, where  $W$  is the total weight for the structure above the isolation system.

Thus, 16 sets of data were computed for a given fixed-base period ( $T_s$ ) and  $\Omega_{0s}$  ratio, source of eccentricity (mass eccentricity or stiffness eccentricity), static eccentricity values and action of the ground motions (unidirectional or bidirectional). For a given combination of static eccentricity, three different actions were considered: unidirectional E-W, unidirectional N-S and bidirectional. Static eccentricities in the superstructure of 5%, 10%, 15% and 20% the floor plan dimension ( $L=21m$ ) were selected, for both one direction and acting on a 45% angle, as depicted in Figures 3 and 4, plus the completely symmetric case ( $e_s=0\%$ ).

Therefore, in order to study the influence of mass and stiffness eccentricities in the superstructure in the torsional response of base isolators of structures for the given  $T_s$  and  $\Omega_{0s}$  parameters, a total of 10,368 simulations were needed for the set of ground motion records considered 21 (Table 2). The 3D-Basis software (Nagarajaiah *et al.* 1991) was used for this purpose. As in previous studies, corner isolators A1, A4, A13 and A16 (Figs. 3 and 4) were selected to monitor the nonlinear response.

#### 6. COMPARISON OF ASYMMETRIC SYSTEMS WITH RESPECT TO SYMMETRIC SYSTEMS

Previous studies (Lee 1980, Nagarajaiah *et al.* 1993) have shown that when the center of stiffness of the isolation system (CRi) coincides with the center of mass of the structure (CMs), structural torques are reduced to a minimum. Therefore, asymmetric systems with stiffness eccentricities in the superstructure (Fig. 4) are compared to counterpart symmetric systems of reference.

In order to compare the peak displacements experienced by the isolators under study (A1, A4, A13 and A16) when there are no eccentricities in the superstructure with those when there are stiffness eccentricities in the superstructure (asymmetric systems, Figs. 4a and 4b), peak displacements for the isolators of asymmetric systems [ $\Delta_{max}(e)$ ] were divided by those of symmetric systems [ $\Delta_{max}(e=0)$ ]. Both unidirectional (Fig. 4a) and

bidirectional eccentricities (Fig. 4b) were considered.

The curves obtained for unidirectional and bidirectional eccentricities are somewhat similar in shape. Peak displacement ductility demands ( $\mu$ ) were usually detected for bidirectional eccentricity. For space constraints, only the curves where the highest amplification and deamplification factors were detected for bidirectional eccentricity for each ground motion (UNION, SMRZ and TMANZ) are shown for each model (SBA1, SBA2, SBA3 and SBA4). Therefore, they are usually isolators A4 and A13 for UNION and TMANZ stations, and isolators A1 and A16 for SMRZ station. For illustration purposes, only the curves obtained for static eccentricities of 5% and 20% are presented.

Results for SBA1 models are shown in Figure 5. It can be observed that for all corner isolators and considered ground motions, there are practically no amplifications or deamplifications of peak displacements for asymmetric systems with respect to symmetric systems. These results demonstrate the benefit of having base-isolated structures with large  $T_I/T_s$  ratios.

Results for SBA2 models, which  $T_I/T_s$  ratios satisfy the minimum requirements of US guidelines, are shown in Figure 6. Higher amplifications are observed in the curves depicted in Fig. 6 for SBA2 models with respect to those obtained for SBA1 models (Fig. 5). Peak amplification factors of 1.15, 1.38 and 1.05 are respectively observed for stations UNION (isolator A13,  $T_I=3.0s$ ), SMRZ (isolator A16,  $T_I=2.0s$ ) and TMANZ (isolator A4,  $T_I=3.0s$ ). Peak deamplification factors of 0.81, 0.79 and 0.87 are respectively observed for stations UNION (isolator A4,  $T_I=1.5s$ ), SMRZ (isolator A1,  $T_I=1.5s$ ) and TMANZ (isolators A4 and A13,  $T_I=1.9s$ ).

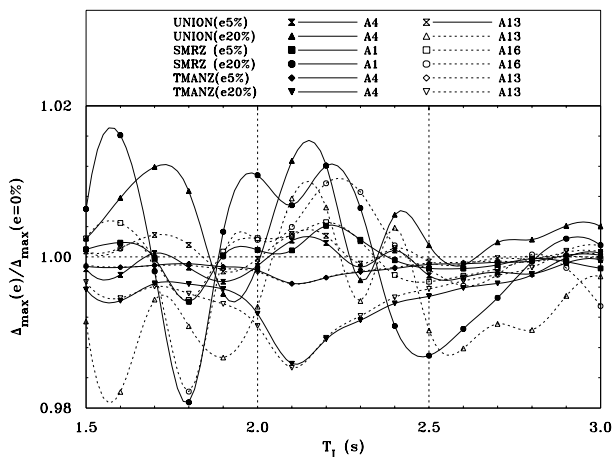


Figure 5.  $\Delta_{\max}(e)/\Delta_{\max}(e=0\%)$  ratios for SBA1 models

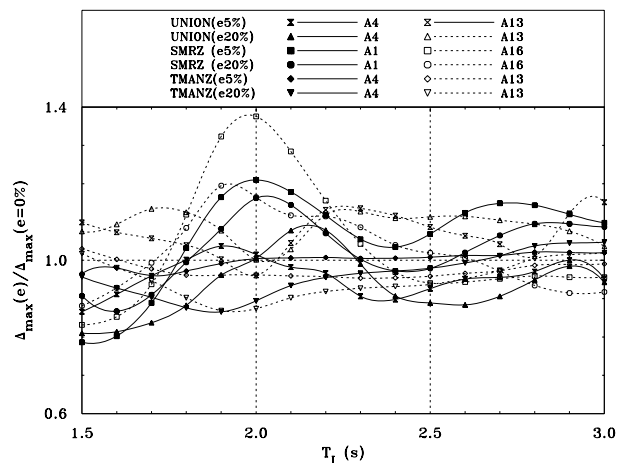


Figure 6.  $\Delta_{\max}(e)/\Delta_{\max}(e=0\%)$  ratios for SBA2 models

Results for SBA3 models, which  $T_I/T_s$  ratios satisfy the minimum recommendation of the New Zealand practice, are shown in Figure 7. Peak amplification factors of 1.29, 1.18 and 1.20 are respectively observed for stations UNION (isolator A13,  $T_I=2.5s$ ), SMRZ (isolator A1,  $T_I=2.0s$ ) and TMANZ (isolator A4,  $T_I=2.7s$ ). Peak deamplification factors of 0.84, 0.75 and 0.80 are respectively observed for stations UNION (isolator A4,  $T_I=1.5s$ ), SMRZ (isolator A16,  $T_I=2.8s$ ) and TMANZ (isolator A13,  $T_I=1.7s$ ). It is worth noting that higher amplifications are observed in the curves depicted for UNION and TMANZ stations for SBA3 models with respect to those obtained for SBA2 models (Figure 6). However, smaller amplifications are observed for SMRZ station for SBA3 model (Fig. 7) with respect to SBA2 model (Fig. 6).

Results for SBA4 models, which dynamic properties are similar to the model previously studied by Nagarajiah *et al.* (1993) where they obtained the highest torsional amplifications, are shown in Figure 8. Peak amplification factors of 1.91, 1.25 and 1.36 are respectively observed for stations UNION (isolator A4,  $T_I=3.0s$  and  $e_s=15\%$ , not shown), SMRZ (isolator A1,  $T_I=1.6s$ ) and TMANZ (isolator A4,  $T_I=2.0s$   $e_s=15\%$ , not shown). Peak deamplification factors of 0.66, 0.75 and 0.79 are respectively observed for stations UNION (isolator A13,  $T_I=2.1s$ ), SMRZ (isolator A16,  $T_I=1.5s$ ) and TMANZ (isolator A13,  $T_I=3.0s$ ).

It is worth noting that, in general, higher amplifications are observed in the entire period range of interest for the curves obtained for SBA4 models (Fig. 8) than for the remaining models (Figs. 5 to 7), perhaps with the exception of SMRZ station for SBA2 model in the period range  $1.8s \leq T_1 \leq 2.3s$  (Fig. 6).

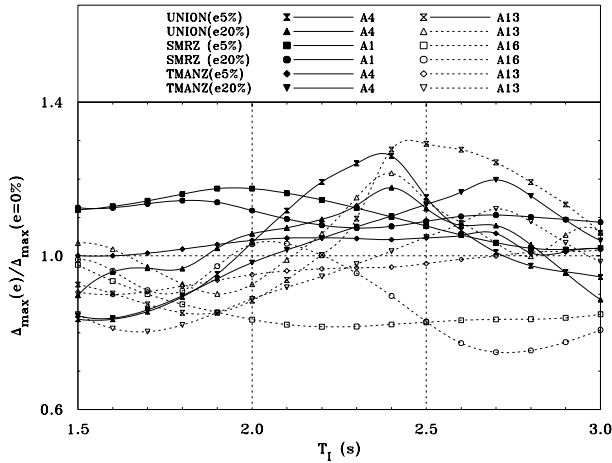


Figure 7.  $\Delta_{\max}(e)/\Delta_{\max}(e=0\%)$  ratios for SBA3 models

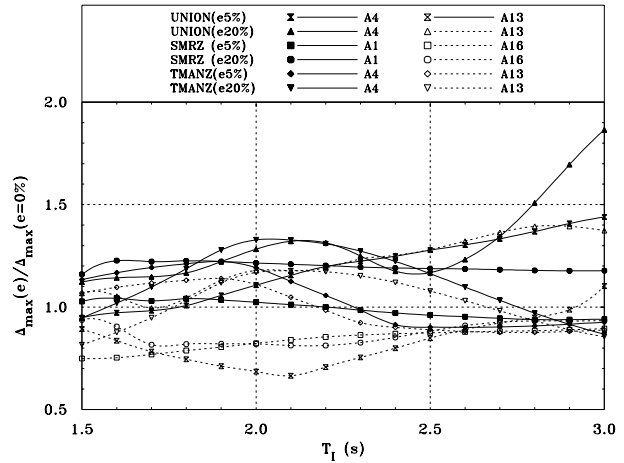


Figure 8.  $\Delta_{\max}(e)/\Delta_{\max}(e=0\%)$  ratios for SBA4 models

## 7. STIFFNESS ECCENTRICITIES VS MASS ECCENTRICITIES

In order to compare the peak displacements experienced by the isolators under study (A1, A4, A13 and A16) when there are mass eccentricities in the superstructure (Fig. 3) with those where there are stiffness eccentricities in the superstructure (Fig. 4), peak displacements for the isolators of asymmetric systems with mass eccentricities [ $\Delta_{\max}(\text{SBAiM})$ ] were divided by those of asymmetric systems with stiffness eccentricities [ $\Delta_{\max}(\text{SBAi})$ ]. Further details of this study are given in Escamilla-Cruz (2005) and Tena-Colunga and Escamilla-Cruz (2007), as for space constraints, few results will be presented and discussed.

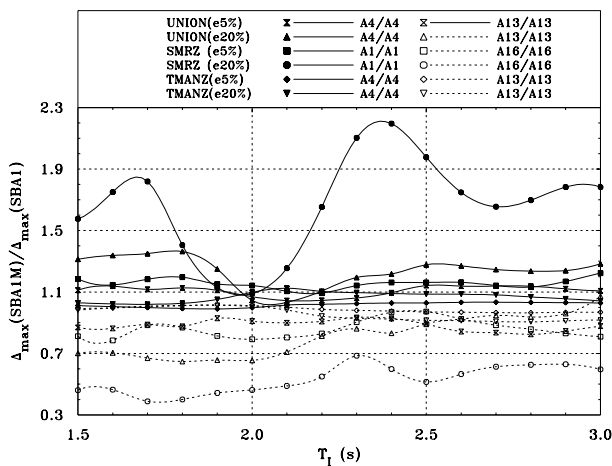


Figure 9.  $\Delta_{\max}(\text{SBA1M})/\Delta_{\max}(\text{SBA1})$  ratios

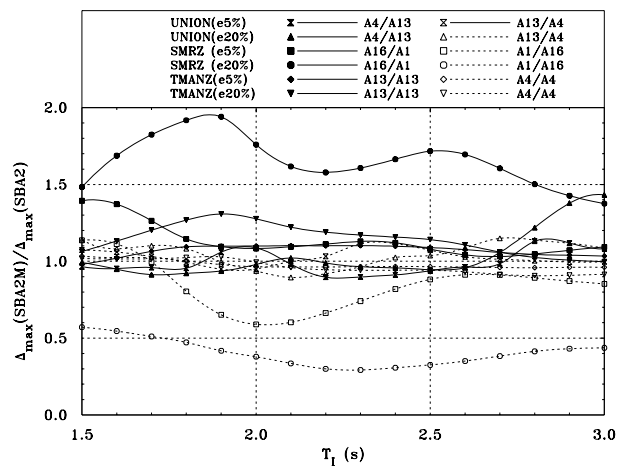


Figure 10.  $\Delta_{\max}(\text{SBA2M})/\Delta_{\max}(\text{SBA2})$  ratios

Results for SBA1 and SBA1M models are shown in Figure 9. Important amplifications and deamplifications are observed for asymmetric systems with mass eccentricities with respect to asymmetric systems with stiffness eccentricities, particularly for station SMRZ. Therefore, it seems that the benefit of having base-isolated structures with large  $T_1/T_s$  ratio to reduce torsional amplifications is restricted to systems with stiffness eccentricities in the superstructure. Peak amplification factors of 1.38, 2.2 and 1.13 are respectively observed for stations UNION (isolator A4,  $T_1=1.8s$ ), SMRZ (isolator A1,  $T_1=2.4s$ ) and TMANZ (isolator A4,  $T_1=2.1s$ ). Peak

deamplification factors of 0.65, 0.39 and 0.90 are respectively observed for stations UNION (isolator A13,  $T_I=1.8s$ ), SMRZ (isolator A16,  $T_I=1.7s$ ) and TMANZ (isolator A13,  $T_I=2.8s$ ). Results for the models which  $T_I/T_s$  ratios satisfy the minimum requirements of US guidelines are shown in Figure 10. Peak amplification factors of 1.45, 1.95 and 1.30 are respectively observed for stations UNION (isolator A4,  $T_I=3.0s$ ), SMRZ (isolator A16,  $T_I=1.9s$ ) and TMANZ (isolator A13,  $T_I=1.9s$ ). Peak deamplification factors of 0.90, 0.30 and 0.90 are respectively observed for stations UNION (isolator A13,  $T_I=2.1s$ ), SMRZ (isolator A1,  $T_I=2.3s$ ) and TMANZ (isolator A4,  $T_I=2.9s$ ).

## 8. CONCLUDING REMARKS

Based upon the parametric study for the bilinear isolators briefly described in this paper and presented in detail by Escamilla-Cruz (2005), one can do the following observations:

- Amplifications (or deamplifications) on the response of asymmetric systems with respect to symmetric systems usually increase as the  $T_I/T_s$  ratio decreases.
- Asymmetric systems with mass eccentricities experience very important amplifications and deamplifications with respect to asymmetric systems with stiffness eccentricities for all models under study.

Therefore, it can be concluded from all these observations that a higher torsional amplification exist in base-isolated structures with mass eccentricities in the superstructure than in base-isolated structures with stiffness eccentricities in the superstructure. This observation is in agreement with what it was found in previous studies (Lee 1980, Nagarajaiah *et al.* 1993) which used a reduced number of effective periods for base-isolated structures ( $T_I$ ) and  $T_I/T_s$  ratios.

## REFERENCES

- Escamilla-Cruz, J. L. (2005). Respuesta torsional de aisladores sísmicos debida a excentricidades de los centros de rigidez de la superestructura. *MSc. Thesis*, Sección de Estudios de Posgrado e Investigación, Escuela Superior de Ingeniería y Arquitectura, Instituto Politécnico Nacional, Unidad Zacatenco, April (in Spanish).
- Lee, D. M. (1980). Base isolation for torsion reduction in asymmetric structures under earthquake loading. *Earthquake Engineering and Structural Dynamics*, 8, 349-359.
- Nagarajaiah, S., Reinhorn A. M. and Constantinou, M. C. (1991). 3D-Basis: Non-linear dynamic analysis of three-dimensional base isolated structures: Part II. *Technical Report NCEER-91-0005*, National Center for Earthquake Engineering, State University of New York at Buffalo.
- Nagarajaiah, S., Reinhorn A. M. and Constantinou (1993). Torsion in base isolated structures with elastomeric isolation systems. *ASCE Journal of Structural Engineering*, **119:10**, 2932-2951.
- Tena-Colunga, A. and Pérez-Osornio, M. A. (2002). Impact of shear deformations on the location of the centers of torsion of shear wall buildings. *Proceedings, Seventh US National Conference on Earthquake Engineering (7NCEE)*, Boston, Massachusetts, CD-ROM, Paper No. 193, July.
- Tena-Colunga, A. and Gómez-Soberón, L. A. (2002). Torsional response of base-isolated structures due to asymmetries in the superstructure. *Engineering Structures*, **24:12**, 1587-1599.
- Tena-Colunga, A (2005). Development of guidelines for the seismic design of base isolated structures in Mexico. *Proceedings, 9th World Seminar on Seismic Isolation, Energy Dissipation and Active Vibration Control of Structures*, Kobe, Japan, June, CD-ROM.
- Tena-Colunga, A. and Zambrana-Rojas, C. (2006). Dynamic torsional amplifications of base-isolated structures with eccentric isolation system. *Engineering Structures*, **28:1**, 72-83.
- Tena-Colunga, A. and Escamilla-Cruz, J. L. (2007). Torsional amplifications in asymmetric base-isolated structures. *Engineering Structures*, **29:2**, 237-247.